CETRA2024 15-17 May 2024, Cavtat, Croatia
8th International Conferenceon Road and Rail Infrastructure

TIRE/PAVEMENT FRICTION: PRESENTATION OF A COMPREHENSIVE PHYSICAL TOOL THROUGH ADVANCED CONTACT MODELLING

Malal Kane
University Gustave Eiffel, Campus de Nantes, AME/EASE, France

Abstract

This paper presents a novel numerical tool for predicting tire/road friction by modeling the tire/road contact dynamics. Incorporating a comprehensive range of influential parameters related to tire properties, road conditions, contaminants, and contact operating conditions, the tool offers a holistic approach to friction estimation. Validation of the tool is achieved through braking tests conducted on a passenger car across a spectrum of speeds and diverse wet road surfaces exhibiting varying textures. The tool effectively ranks the friction coefficients associated with ABS (peak friction) and locked-wheel (sliding friction) conditions on these varied road surfaces, affirming its accuracy and utility in assessing tire/road interactions.

Keywords: pavement friction, contact modeling, skid resistance, tire-road interaction, predictive tool

1 Introduction

The braking and obstacle-avoidance capabilities of vehicles rely on the grip between their tires and the road surface [1]. This grip is essential for generating sufficient frictional forces during maneuvers, ensuring safety [2]. However, predicting these friction forces is challenging due to various factors such as road conditions, tire properties, contaminants, and vehicle operating conditions. Existing models for friction prediction are often empirical, requiring numerous tests and limited in their applicability beyond tested ranges, making them costly and impractical [3, 4].

To address this limitation, a comprehensive physical model that captures the intricate nature of friction force generation is proposed [5, 6]. The model considers all relevant parameters associated with tires, road surfaces, contaminants, and operating conditions. Specifically, a visco-elasto-hydro-rough contact model to accurately simulate tire-pavement interaction is adopted.

With this advanced tool, I aim to enhance friction force predictions across a broader range of conditions while minimizing costs associated with testing. This tool promises to improve safety and efficiency in vehicle operation by providing more accurate insights into tire-road interactions.

DOI: https://doi.org/10.5592/CO/CETRA.2024.1537

2 The tool

2.1 Modeling

The foundational principle of the tool lies in quantifying the friction generated within the wet contact path between a rotating tire, operating at a specified speed and slip ratio, and a textured road surface. Frictional forces are presumed to stem from hysteresis and adhesion mechanisms, modulated by the hydrodynamic influence of a lubricating layer [6]. The computational framework comprises two primary steps: The initial step involves determining the overall deformation of the loaded tire, consequently establishing the apparent contact area. This step operates at the scale of the tire structure and is executed in a static mode, considering the road surface as smooth and rigid. Key inputs include the tire diameter, normal load, and an "equivalent structural stiffness" parameter, which is intricately linked to the tire's inflation pressure and carcass stiffness. Further details regarding the computation of this global deformation are elucidated in the "Calculation Algorithm" section. Subsequently, the deformed tire is overlaid with its grooved rubber tread, and the entire system is simulated moving across the rough road surface. At this stage, input parameters encompass the load, rubber material behavior laws, tire speed, slip ratio, surface topography, water thickness, among others (refer to Figure 1 (b)).

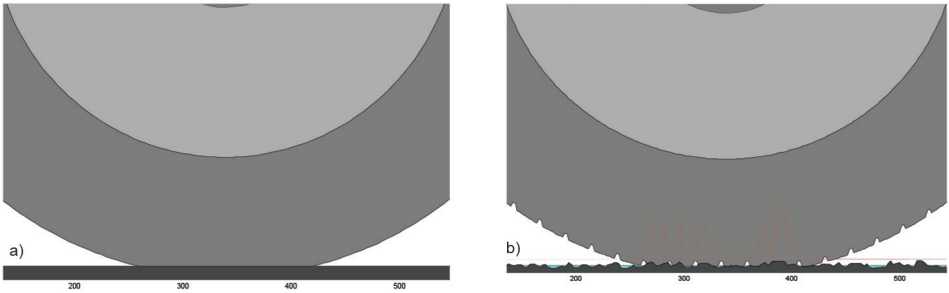

Figure 1 The two calculation steps. The first determines the apparent contact area assuming the tire static and the road smooth (a). The second step determines the real contact area and thus the friction with the moving tire tread patterned on the rough road surface (b).

The governing equations (Equations 1 to 8) are derived from the balance of forces acting within the contact area [6]. The indices i and j respectively denote a tread element and a road element. For an ith moving tread element in contact with the jth static road element, Equation 1 represents the equilibrium of forces (refer to Figure 2).

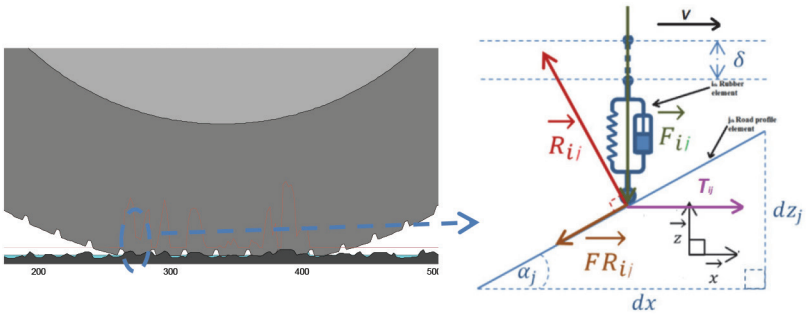

Figure 2 Forces acting between rubber and road profile elements

$$\vec{F_{ij}} + \vec{T_{ij}} + \vec{R_{ij}} + \vec{FR_{ij}} = \vec{o} \quad (1)$$

Refer to [6] for the other element signification of the equation 1. FRij is a local friction force, defined as μlocRij when the element is moving on a "pseudo smooth inclined plane" with angle αj. μloc corresponds to a local friction coefficient reflecting the actual adhesion coefficient (which is negligible in wet conditions) and/or a local hysteresis coefficient that accounts for the contribution of asperities with wavelengths smaller than the resolution at which the surface texture is captured. Figure 3 illustrates the multiscale representation of the local scale from larger to smaller resolutions.

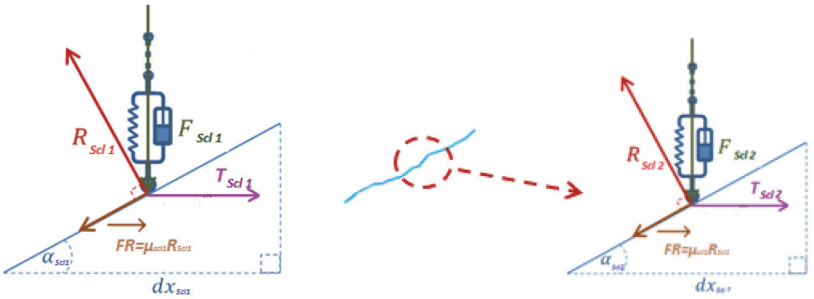

Figure 3 Fractal representation of the local hysteretic contribution of all texture scales smaller than the resolution with which the profile is recorded- From left to right, larger to finer scales (here, scales 0 to 2 are illustrated)

The projection of Equation 1 onto the x and z axes, coupled with the condition $FR_{ij} = \mu_{loc} R_{ij}$ leads to:

$$T_{ij}(t) = F_{ij}(t) \frac{\sin(\alpha_j) + \mu_{loc}\cos(\alpha_j)}{\cos(\alpha_j) - \mu_{loc}\sin(\alpha_j)} \quad (2)$$

When a tread element is not in contact with the road surface, its contact pressure is zero, and the element enters a relaxation phase. Its position on the Z-axis is then determined by solving the following equation:

$$Ku_{ij}(t) + C\frac{du_{ij}(t)}{dt} = o \quad (3)$$

At any time t, the total load W applied by the tire on the road surface must be balanced by the normal contact pressure:

$$W = \sum_{i}^{N} F_{ij}(t) \quad (4)$$

Where N is the number of elements comprising the tire tread in the contact area. Accordingly, the global friction coefficient $\mu_j(t)$ can then be calculated using the following formula:

$$\mu_j(t) = \frac{\sum_{i}^{N} T_{ij}(t)}{W} \quad (5)$$

At this stage, the only unknown factors are $F_{ij}(t)$, representing the distribution of the contact forces applied by the tread to the road surface [6].

2.2 Introducing the slip rate

The slip rate τ is introduced during the rotation of the tire via the relative positioning of the rubber and road elements. Assuming the tire is moving on the surface at speed V and a slip ratio τ, if at time t, the rubber element i is in contact with the road element j, then at time t+dt, the position of the rubber element i would be:

$$ij = +\tau \times V \frac{dt}{dx} \tag{6}$$

2.3 Lubricating the contact (wetting)

The hydrodynamic pressure exerts a lift-up force on the tread, thereby reducing its penetration depth into road asperities. To incorporate this phenomenon, we adopt a simplification known as the "pseudo-hydrodynamic bearing," where we calculate its "hydrodynamic bearing capacity" W_h.

$$W_h = \frac{\alpha 6 n V^{\beta} l L^2}{H_{out}^2 (a-1)^2} \left[\log(a) - 2\frac{a-1}{a+1} \right] \tag{7}$$

Where, , with and are respectively the outlet and inlet water thicknesses of the "pseudo hydrodynamic bearing". is the water viscosity. L and l are the lengths and the width of the apparent tire/road contact area. α and β are two empirical coefficients [1].

2.4 Tool inteface

Table 1 provides a summary of the inputs required for the model, encompassing parameters associated with the tire, road, contaminant, and operating conditions. Figure 4 depicts the interface of the numerical calculation program.

Table 1 Inputs of the model

Tire	Road surface	Contaminant	Op. condi.
Tire dimensions (Width and Diameter), Tread depth, Carcass stiffness, Stiffness and Viscosity	Surface profile, Resolution, Adhesion coefficient	Density, Viscosity, thickness	Normal load, Speed, Slip ratio

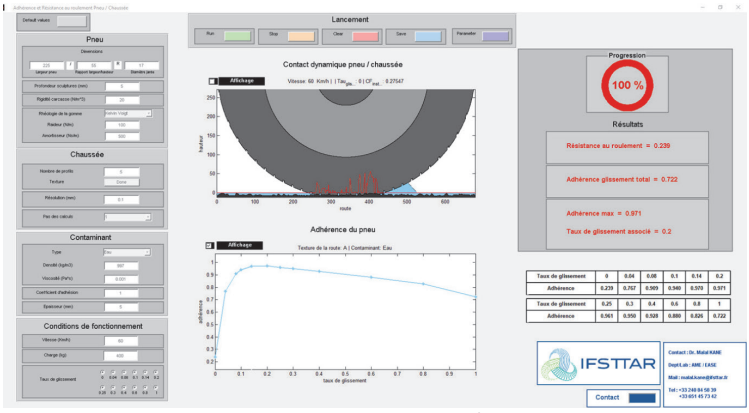

Figure 4 General tool interface for calculating the tire/road friction

3 Experimental device

3.1 Road surfaces

The test surfaces are situated within the university's test track on the campus of Nantes. These surfaces feature a diverse array of microtexture and macrotexture scales, providing varying levels of grip. Figure 5 (a) presents the names and illustrations of these surfaces, accompanied by details of the materials utilized. Additionally, Table 2 presents the indirect values of microtexture (measured by DFT at 20 km/h [6]) and macrotexture via MPD (Mean Profile Depth [7]), thereby showcasing the diversity of the tested surfaces through the combination of these two parameters.
To integrate these surfaces into the simulation tool, their textures are captured using a profilometer. Specifically, 12 parallel profiles, each measuring 1200 mm in length with a resolution of 0.1 mm, are systematically distributed across a width of 350 mm on each surface. These profiles are precisely taken along the path where the instrumented tire of the test vehicle traverses during surface testing. Figure 5 (b) illustrates an example of one of the considered profiles.

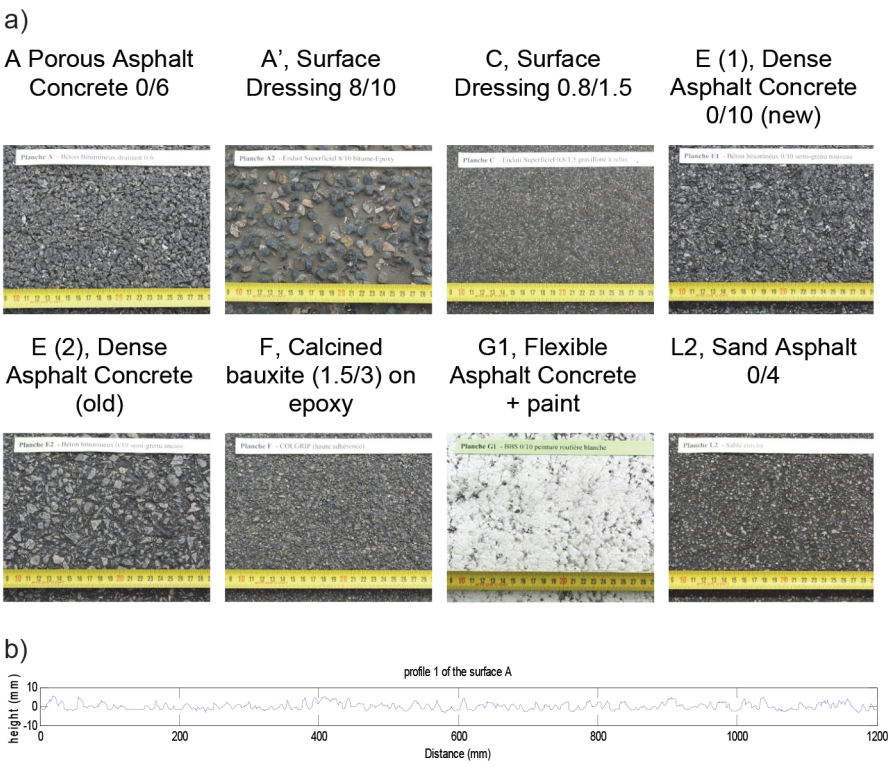

Figure 5 a) Test surfaces, b) Example of a captured profile

Table 2 The indirect values of microtexture (measured by DFT at 20 km/h) and macrotexture via MPD (Mean profile deep) of the tested surfaces

Pavement surface	MPD	DFT @ 20 km/h
E1	0,744	0,639
C	0,632	0,779
L2	0,618	0,64
G1	0,461	0,246
F	1,566	1,006
Go	0,676	0,678
E2	1,001	0,557
A	1,146	0,642
A'	3,4575	0,655

3.2 Test procedure

For each test, the following standardized procedure is adhered to: The track undergoes an initial watering process using a system of strategically positioned nozzles along its length. Watering is terminated upon reaching a targeted thickness range of 1 to 2 mm. Subsequently, the watering process is halted, and the braking test ensues. The test is conducted with the vehicle speed maintained at a consistent 60 km/h. Once the vehicle is positioned on the designated surface, the driver initiates the braking procedure.
The test vehicle utilized is a Clio 3 (refer to Table 3 for specifications). Equipped with sensors providing data on forces and torques in three directions at the right front wheel, as well as the speed of the car and each wheel (see Figure 6), the vehicle ensures accurate measurements throughout the test.

Table 3 Test car characteristics

Model	Renault Clio 3
Power	112 Cv (82 KW)
Weight	1485 kg
Wheelbase	2,575 m
Larger	1,72 m
Weight (front wheels)	858 kg
Inflation Pressure (front)	2,2 bars
Inflation Pressure (rear)	2,0 bars

During each test iteration, the same protocol is meticulously followed: maintaining the initial speed, the driver applies the brakes with or without ABS once the car is on the appropriate surface. Upon reaching the predetermined final speed, the driver releases the braking system.

Figure 6 Instrumented Clio 3 Setup for Braking Tests

4 Validation of the tool

4.1 Relevancy of the model

Figure 7 (a) illustrates a typical 3D plot of experimental friction results versus slip ratio and speed [5]. In Figure 7 (b), results of simulations conducted with the tool using inputs corresponding to the same operating conditions as the aforementioned experiments are presented. Although the surface used in the simulations differs from that of the experiments (profiles of surface A were utilized due to availability), the two 3D curves exhibit a similar trend. Both plots demonstrate the characteristic behavior of friction coefficients, with the maximum typically occurring between 10% and 20% of the slip rate, followed by a decline. Moreover, the simulations effectively replicate the decrease in the friction coefficient with increasing speed during locked-wheel conditions. This agreement between experimental and simulated results underscores the relevance and accuracy of the model in capturing the essential dynamics of tire-road interactions.

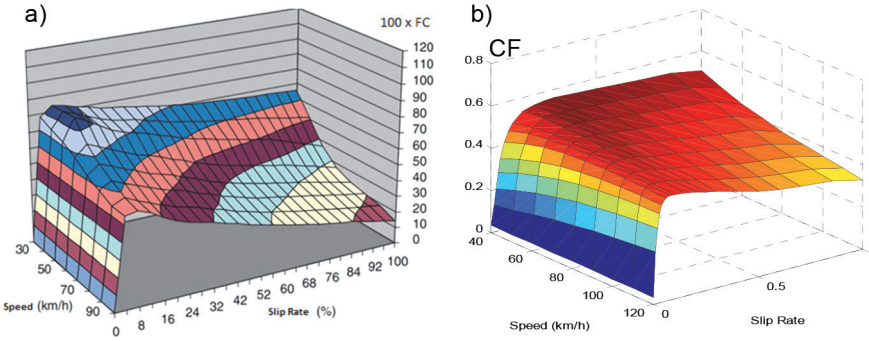

Figure 7 The (a) and (b) display typical examples of tire/road friction coefficient variation against the slip ratio and speed respectively from experimental results [5] and calculated with the model

4.2 Comparison between infield tests and the tool predictions

Figure 8(a) and (b) depict the peak frictions (red bars) and sliding frictions (green bars), respectively, predicted by the tool and observed in tests conducted on eight surfaces. Primarily, the ranking of surfaces in terms of peak and sliding frictions aligns between the model and the experiments, except the sliding frictions of surface A. However, it's notable that the model values are approximately half of the corresponding experimental values.

This discrepancy in model values can be attributed to the relatively low capture resolution of the surfaces, which at 100 µm, leaves a significant portion of the microtexture unaccounted for in the captured profiles. Particularly for surfaces with higher microtexture, such as F and A, where a substantial portion of the microtexture is not captured (refer to Figure 9), the tendency of the tool to predict lower values is accentuated. Improved results from the tool could likely be achieved by increasing the capture resolution of surfaces during profiling.

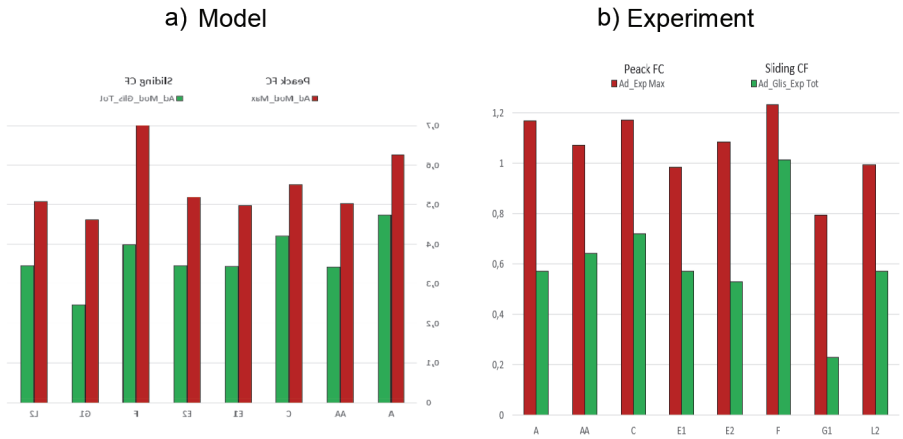

Figure 8 Peak-frictions and sliding-frictions on different test surfaces

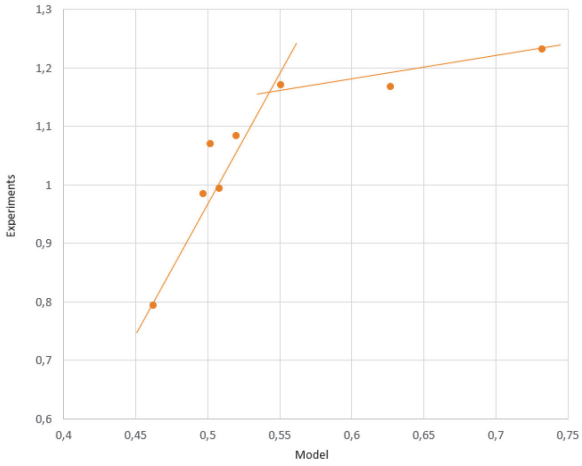

Figure 9 a) - Model (100 µm of surface resolution), b) - Experiments (Braking tests)

5 Conclusion

This paper introduced the development of a comprehensive tool for estimating tire/road friction, which meticulously considers all parameters about tire, road, and contact operating conditions. For the tire, the tool incorporates geometrical aspects, rubber material properties, and tread patterns. Regarding the road, it accounts for surface texture and contaminant conditions, including lubricant depth, viscosity, and density. Operating conditions are addressed through parameters such as load, speed, and slip ratio of the tire.

The tool's validation involved conducting braking tests with a passenger vehicle at varying speeds on wet roads with different textures. While areas for improvement remain, the trend of the predicted results closely resembled those obtained in experimental testing.
An avenue for enhancement lies in determining the appropriate resolution for capturing road surfaces. Additionally, given the limitations of current in-situ profilometers, which cannot achieve resolutions below 100 µm, consideration must be given to how these uncaptured scales can be incorporated into simulations through µloc. This underscores the ongoing quest for refining and advancing the tool's capabilities to better simulate real-world tire/road interactions.

References

[1] Ong, G.P., Fwa, T.F.: Mechanistic interpretation of braking distance specifications and pavement friction requirements, Transportation Research Record, 2155 (2010) 1, pp. 145-157

[2] Najafi, S., Flintsch, G.W., Medina, A.: Linking roadway crashes and tire–pavement friction: A case study, International Journal of Pavement Engineering, 18 (2017) 2, pp. 119-127

[3] Lacombe, J.: Tire model for simulations of vehicle motion on high and low friction road surfacesm, 2000 Winter Simulation Conference, pp. 1025-1034, Orlando, FL, USA, 10-13 December 2000.

[4] Yi, K., Hedrick, K., Lee, S.C.: Estimation of tire-road friction using observer based identifiers, Vehicle System Dynamics, 31 (1999) 4, pp. 233-261

[5] Kane, M., Edmondson, V.: Tire/road friction prediction: Introduction a simplified numerical tool based on contact modelling, Vehicle system dynamics, 60 (2022) 3, pp. 770-789

[6] Kane, M., Do, M.T., Cerezo, V., Rado, Z., Khelifi, C.: Contribution to pavement friction modelling: an introduction of the wetting effect, International Journal of Pavement Engineering, 20 (2017) 8, pp. 965-976, DOI: 10.1080/10298436.2017.1369776